Yield Stress of Mixed Suspension of Silica Particles and Lysozymes: The Effect of Zeta Potential and Adsorbed Amount

Atsushi Yamaguchi[a], Motoyoshi Kobayashi[b,*], and Yasuhisa Adachi[b]

[a]Graduate School of Life & Environmental Sciences, University of Tsukuba
1-1-1 Tennoudai, Tsukuba, Ibaraki 305-8572, Japan
[b]Faculty of Life & Environmental Sciences, University of Tsukuba
1-1-1 Tennoudai, Tsukuba, Ibaraki 305-8572, Japan

*Corresponding author
E-mail: kobayashi.moto.fp@u.tsukuba.ac.jp
Tel & Fax: +81-(0)29-853-5721

Conflict of interest

The authors declare that they have no conflict of interest associated with this article.

Abstract

To investigate the interactions between colloidal particles in the presence of oppositely charged proteins, the yield stress of a mixed suspension of silica particles and lysozymes was measured as a function of lysozyme dose and pH. Further, the corresponding surface properties of silica particles covered with lysozymes were determined by measuring the adsorbed lysozyme amount and zeta potential. The present results indicated that an increase in the adsorbed lysozyme amount increases the zeta potential of silica particles from negative to positive through an isoelectric point. As expected from the Derjaguin–Landau–Verwey–Overbeek (DLVO) theory, the maximum value of yield stress is obtained around the isoelectric point and the yield stresses decrease with an increase in the zeta potential magnitude. However, the maximum yield stress depends on the pH, and yield stresses at the same zeta potential magnitude are different depending on the zeta potential sign even if the pH values are similar. That is, the relationship between yield stress and zeta potential is asymmetric with respect to the isoelectric point. These asymmetric results of the yield stress indicate the existence of non-DLVO forces, such as patch-bridging attraction and lateral repulsion between adsorbed lysozymes, affected by the adsorbed amount of lysozyme. Our analysis suggested that the relative adsorbed amount, defined as the ratio of the adsorbed amount to the maximum adsorbed amount, can be used as a parameter to explain the asymmetric feature of the yield stress with respect to the zeta potential. In addition to the zeta potential, the surface occupation of adsorbed substances is critical in controlling particle–particle interactions.

Key words: Non-DLVO force; Surface coverage; Rheology; Proteins; Patch-bridging

1. Introduction

Interactions between particles in a colloidal suspension govern the stability and rheological properties of the suspension. In a mixed suspension of colloidal particles and proteins, adsorbed proteins change particle–particle interactions by modifying the particle surface through adsorption. Hence, they are crucial in several industries, including pharmaceutical, cosmetic, food, and environmental industries, for understanding the mechanism of particle–particle interactions in the presence of proteins [1–3].

Particle–particle interactions are often discussed based on the Derjaguin–Landau–Verwey–Overbeek (DLVO) theory [4,5]. The DLVO theory suggests that the total interactions can be obtained by summing the electric double layer and the van der Waals forces. The validity of the DLVO theory is confirmed by direct force measurements [6,7] as well as indirect techniques, such as measuring the aggregation rate and yield stress [8–11]. Moreover, additional non-DLVO interactions, which are not included in the DLVO theory, are sometimes observed, especially in colloidal suspensions comprising more than two materials [12–21].

When one considers the interactions between colloidal particles in the presence of proteins, one can refer to studies on the mixtures of colloidal particles and other materials, such as polymers, polyelectrolytes, and surfactants. These materials are typically adsorbed on particles and cause non-DLVO interactions [12–21]. Well-known mechanisms of non-DLVO interactions include patch, bridging, steric, and hydrophobic interactions. Smellie and La Mer [22] introduced a simple consideration based on the bridging. They proposed that occupied and unoccupied surface fractions govern the probability of bridging formation. Thus, the probability of bridging is proportional to $\theta(1-\theta)$, where θ refers to the surface coverage. Zhao et al. [23] reported that the attraction between polystyrene microspheres coated with poly(N-isopropylacrylamide) microgels is the maximum when the ratio of the adsorbed amount to the maximum adsorbed amount under the same solution conditions was nearly 0.5. Although they did not examine the electric properties of the materials as they had focused on hydrophobic interactions, their results clearly indicated the dependence of particle–particle interactions on the adsorbed amount. According to the Smellie and La Mer concept, it is implicitly assumed that a surface can be completely covered by adsorbates. In the case of charged substances, however, the maximum surface coverage is often significantly less than the highest possible adsorption owing to electric repulsion between the adsorbed substances [24–27]. Thus, the applicability of Smellie and La Mer's concept on charged substances may be limited.

The effects of the electric properties of materials on particle–particle interactions are often studied in the presence of oppositely charged polyelectrolytes [12,17–20]. The adsorption of oppositely charged polyelectrolytes onto colloidal particles induces charge neutralization and overcharging. The net charge of a particle is reduced or reversed by the adsorption of opposite charges from polyelectrolytes. Additionally, patch, bridging, and steric interactions may occur. These interactions should depend on the

amount of adsorbed substances. However, systematic and quantitative studies on the effect of the adsorbed amount of charged substances on particle–particle interactions are scarce.

The silica particle–lysozyme system is widely studied [28–32] because of the high degree of accessibility and usability of both materials for fundamental research and practical use. Lerche and Sobisch [30] used the sedimentation technique and demonstrated that suspensions are stabilized at a low pH although the absolute value of the zeta potential of lysozyme-coated silica nanoparticles is low. Meanwhile, suspensions at a higher pH were destabilized although the absolute values of the zeta potential were relatively high. Nevertheless, we demonstrated in our previous study [32] that a qualitative explanation for the aggregation rate of submicron silica particles in the presence of lysozymes can be partly achieved in terms of the DLVO theory by considering the heterogeneity of surface charges. However, further systematic and quantitative studies are necessary to understand the interactions between silica particles in the presence of lysozymes.

Yield stress measurement is a useful method to investigate particle–particle interactions [10,33]. The yield stress of a suspension depends on the interparticle forces, solid volume fraction, particle size distribution, and particle networks [10,11,33–36]. By choosing and consolidating the sample conditions and preparation method, one can obtain information on interparticle forces directly from the yield stress.

We herein present the measured yield stresses of mixed suspensions of lysozymes and silica particles. Furthermore, the yield stresses are compared with experimentally obtained zeta potentials and adsorbed lysozyme amounts. Interestingly, the yield stress exhibits a DLVO-like interaction regime and a non-DLVO-like regime. The mechanisms of both interaction regimes are discussed in terms of the adsorbed amounts.

2. Materials and Methods

2.1 Materials

Silica particles: In this study, we used commercially available colloidal silica particles (KE-P30, Lot No. 3A15, Nippon Shokubai). The particles were synthesized using a process similar to that reported by Stöber [37]. Silica powder was heated at 800 °C for 24 h before preparing suspensions and storing them in a drying desiccator.

The number average diameter $< d >$ and the standard deviation of the silica particles were measured by transmission electron microscopy (TEM, H7650, Hitachi High-Technologies Corporation). To analyze the average diameter and standard deviation, areas of 800 projected circles of silica particles were measured from micrographs using the ImageJ software and converted into diameters. The average diameter was 302 nm, while the standard deviation was 20 nm.

The specific surface areas were obtained from nitrogen gas adsorption (BET) measurement performed on the SA 3100 instrument (Beckman Coulter) and from TEM micrographs using the relationship $(6/\rho) < d^2 > / < d^3 >$. Here, ρ is the density of the silica particles, which was reported to

be 2.2×10^3 kg/m^3 [37]. The specific surface area, as calculated from TEM, was 9.0×10^3 m^2/kg, while that obtained from BET measurements was 1.25×10^4 m^2/kg.

Lysozymes: Hen egg-white lysozyme (L6876, Sigma Aldrich) was used without further purification. It has been previously reported that a lysozyme is an oval sphere with dimensions of 3 nm × 3 nm × 4.5 nm [27,38,39]. In this study, we assumed the lysozymes to be spheres of 1.7 nm radius, as calculated from the cubic mean radius [31,40]. The molecular weight of the lysozyme was 14.3 kDa. All the lysozyme solutions were used within 2 weeks of preparation. The electrophoretic mobility of the lysozyme is reported elsewhere [39,40] and the isoelectric point (iep) of the lysozymes lies in the pH range of 9–11.

Chemicals and Water: The KCl (JIS special grade, Wako Pure Chemical Industries) solution was used as an ionic strength adjuster. KOH and HCl solutions were used to control the pH. Through the present study, deionized water (Elix Millipore) with an electrical conductivity of approximately 0.07 μS/cm was used to prepare all solutions and suspensions.

2.2 Yield stress

The yield stresses of mixed suspensions of silica particles and lysozymes were measured by the vane method. In the vane method, a vane-type spindle is inserted into a sample and rotated at an extremely low rotational speed. The relation of torque vs. time exhibits the maximum torque when the material yields. As yield stress τ_y is the shear stress when a sample yields, τ_y can be calculated from the maximum torque T_m and spindle dimension by [41,42],

$$T_m = \frac{\pi D^3}{2}\left(\frac{H}{D} + \frac{1}{3}\right)\tau_y, \quad (1)$$

where D and H are the spindle diameter and height, respectively.

The concentration of silica was 50 wt.% and the mass ratio of lysozyme to silica ranged from 0–0.012 g/g. The KCl concentration was maintained at 10 mM. First, the silica particles were placed in the sample bottle after satisfying the requirements for the vane method, as detailed by Dzuy and Boger [41]. Deionized water was added to the sample, subsequently it was shaken vigorously and stored overnight to wet the silica particles. Next, the KCl solution, lysozyme solution, and HCl or KOH were added to the silica suspension after it was sonicated. The total ionic strength of the silica suspension was adjusted to 10 mM with KCl, HCl, and KOH solutions. The sample pH was measured with a combination electrode (6.0234.100, Metrohm). Small amounts of HCl and/or KOH solutions were added to the sample to adjust the pH within an error margin of ±0.1 with respect to the target pH. The sample was subsequently shaken gently for 24 h.

Yield stress measurements were performed with viscometers (LVDV-II+Pro, HADV-II+Pro, BROOKFIELD) with the V-74 vane spindle. To minimize the effect of the sample preparation process, the

following operations were performed before each measurement. The sample suspension was shaken vigorously for 20 s with a vortex mixer (MFG No.6087546, TAITEC) to maintain a uniform floc morphology [43] and left to stand for 2 min. Subsequently, the spindle was inserted into the sample. After 3 min, the measurement was started. The rotational speed of the spindle was 0.1 rpm, and the torque was measured after every 1 s. The yield stress measurements were performed at least five times for each sample at intervals of 10 min. The measurements were performed at 20 °C.

2.3 Zeta potential

The zeta potential of the silica particles covered with lysozymes was measured by the electroacoustic method (DT-1202, Dispersion Technology Inc.). Silica suspensions of 50 g/L (0–0.024 g/g mass ratio of lysozymes to silica particles) were prepared with 10 mM KCl. The pH of the suspensions was adjusted to 5 or 7 with KOH and/or HCl within an error margin of ±0.1. The suspensions were shaken gently for more than 24 h to equilibrate the adsorption of lysozymes. Each measurement was started immediately after gently mixing the suspension to prevent the sedimentation of silica particles. The measurements were performed thrice on each sample; the zeta potential measurements were performed at 25 °C. It is noteworthy that we can compare the results of the zeta potential measurements with those of the yield stress measurements using the mass ratio of lysozymes to silica particles because the number of lysozymes to one silica particle is constant.

2.4 Adsorbed amount

The adsorbed amounts of lysozymes on silica particles were taken from a previous study [32]. In our previous study, the mixed suspension of silica particles and lysozyme at pH 5 and 7 with 10 mM KCl was prepared similarly as that for the zeta potential measurements. The silica particles covered with lysozymes were removed by centrifugation with 20630 g for 5 min at room temperature (20 °C) using a centrifuge equipment (3520, Kubota). The lysozyme concentrations in the supernatants were determined by ultraviolet (UV) absorbance measurements at a wavelength of 280 nm using a spectrophotometer (UV-1650PC, Shimadzu) and the standard calibration curve of absorbance as a function of lysozyme concentration. The adsorbed lysozyme amount was obtained as the difference between lysozyme dose and supernatant concentration.

The surface coverage was calculated from the adsorbed amount by the relation $\theta = 1000 N_{\mathrm{A}} A_{LSZ} \Gamma / (M_w \cdot a_{silica}^{TEM})$. Here, N_{A} is the Avogadro constant; A_{LSZ} is the projected area of the lysozyme, i.e., 9.3×10^{-18} m^2, when the lysozyme is regarded as a sphere with a radius of 1.7 nm; Γ is the adsorbed amount of lysozyme in g/g; M_w is the molecular weight of lysozyme; a_{silica}^{TEM} is the TEM specific surface area of the silica particle. It is noteworthy that A_{LSZ} in this study is the value between projected areas at side-on and end-on adsorptions [27].

3. Results and Discussion

3.1 Surface properties of silica particles covered with lysozymes

The values of zeta potential of the lysozyme-coated silica particles in a 10 mM KCl solution at pH 5 and 7 are plotted against the adsorbed amount and the corresponding surface coverage in Figure 1. The symbols denote the experimental values. The adsorption of lysozyme is almost saturated in this experimental range. That is, a further increase in lysozyme dose does not change the zeta potential and the adsorbed amount significantly. Meanwhile, under both pH conditions, the lysozymes are completely adsorbed on the silica particles until the adsorbed amount reaches almost the maximum value.

Figure 1 shows that the bare silica particles possess negative zeta potentials at both pH values. An increase in the adsorbed lysozyme amount results in a reduced zeta potential magnitude. A further increase in the adsorbed amount results in charge reversal and the zeta potentials of the lysozyme-coated silica particles becoming positive. Finally, the zeta potentials become almost constant at adequately high lysozyme doses and the adsorbed lysozyme amount becomes saturated (see Figure S1 in Supporting Information). The iep at pH 5 is found at a lower lysozyme dose than that at pH 7 because silica particles have lower negative charge density, while lysozymes exhibit a strong positive charge at pH 5.

The maximum adsorbed amount at pH 7 is 4.2 times larger than that at pH 5. These trends have been reported elsewhere as well [27–29,31]. We consider that the dependence of the adsorbed amount on pH can be understood in terms of the three-body random sequential adsorption (RSA) model that considers the electrostatic forces between lysozymes and those between a lysozyme and silica surface [24,25]. According to the three-body RSA model, at pH 5, the strong positive charge of the lysozymes and the weak negative charge of the silica particles result in a strong lateral repulsion between the lysozymes and, hence, decreases the maximum adsorbed amount. Further, at pH 7, the weak positive charges on the lysozymes and the strong negative charges on the silica particles result in a weak lateral repulsion between the lysozymes and in a large maximum adsorbed amount.

3.2 Results of yield stress measurement

The yield stress is plotted against the adsorbed amount and corresponding surface coverage in Figure 2. The symbols represent experimental values in 10 mM KCl at pH values of 5 and 7. The lines correspond to the yield stresses of silica suspensions without lysozyme in 0.5 M KCl, where electrostatic repulsions should be ineffective [32]. Here, the adsorbed amounts are interpolated from the experimental values. Under both pH conditions, an increase in the adsorbed amount results in an increase in the yield stress until it reaches the maximum value. Subsequently, the yield stresses decrease with an increase in the adsorbed amount. The maximum yield stress at pH 5 is located at a lower adsorbed amount of lysozymes than that at pH 7. These results agree well with the zeta potential measurements shown in Figure 1.

The yield stresses of the suspensions are plotted against the zeta potentials of silica particles covered with lysozymes, as shown in Figure 3. The horizontal line is the yield stress of the bare silica

particle suspension with 0.5 M KCl. The vertical line is the zeta potential, where the relative adsorbed amount (which is discussed in the fifth section at section 3.3) is equal to 0.5. The pictures above are a schematic representation of the gap between silica particles. Here, the zeta potentials are interpolated from the experimental values (see Figure S1). As expected from the DLVO theory and previous studies, a strong correlation exists between the experimental results of yield stress and zeta potential. In other words, Figure 3 shows that, under both pH conditions, the maximum yield stresses are located around the iep, and increasing the magnitude of the zeta potential decreases the yield stress. These trends are explained in terms of the classical DLVO theory. In simple terms, large yield stresses around the iep are caused by the van der Waals attractive forces and a weak electric repulsion between silica particles. Moreover, increasing the magnitudes of the zeta potentials increase the electric repulsion between the silica particles, and a large electric repulsion results in a lower yield stress.

Some trends in Figure 3 can be explained in terms of the DLVO theory. Nevertheless, other trends cannot be explained unless non-DLVO forces are considered. First, the maximum yield stress depends on the pH. Next, under both pH conditions, the maximum yield stresses of the mixed suspensions of lysozymes and silica particles are larger than the yield stresses of bare silica suspensions in 0.5 M KCl, where electric repulsions do not come into play. Furthermore, the graph is not symmetrical with respect to the iep especially at pH 7. That is, the magnitude of the yield stress depends on the pH and zeta potential sign. The yield stresses are different even at the same magnitude of zeta potential if the sign is different. This indicates the importance of the surface coverage effects that are not reflected in the zeta potential.

3.3 Discussion on the mechanisms of non-DLVO forces

When one considers the mechanisms governing the maximum yield stress at each pH, the specific feature of the flocculation of silica particles must be considered. Figure 4 shows the yield stress of silica suspension without lysozymes in 0.5 M KCl. Low yield stresses are observed under conditions of low pH; this observation is similar to previously reported results [43]. The low yield stress at low pH values is considered to be due to repulsive forces between the hairy or gel-like structures on silica surfaces [37,44], or the reduction in additional attractions by ion–ion correlation [43]. This specific feature of silica particles should be the contributing factor to the pH dependence of the maximum yield stress of mixed suspensions of silica particles and lysozymes. Furthermore, large errors at pH 6 and 7 are observed. We infer that this is caused by the instability of the suspension. The specific hindering of aggregation of bare silica particles occurs at a low pH and the boundary between the aggregation and dispersion regimes is located at pH 6–7 [44]. Therefore, we consider that the suspensions around pH 6–7 are unstable and affected easily by the small difference in pre-treatment prior to each measurement.

Kobayashi et al. [37,44] demonstrated that the aggregation rate of silica particles decelerated at low pH values or when the particle size was small. Such specific hindering of aggregation can be suppressed by heating. Furthermore, in our previous study, we used the same particles with heating as those used in

this study, and demonstrated that the aggregation rate in the fast aggregation regime was independent of pH [32]. Additionally, in the present study, a decrease in the yield stress is observed at low pH values although the silica particles are heated before experimentation. We theorize that this contradiction between the yield stress and aggregation rate is owing to the difference in characteristic distances that affect each phenomenon. That is, the characteristic distance for aggregation may be larger than that for yielding because aggregation is an approaching process, while yielding is the broken retracting process of floc [15]. Thus, the aggregation rate may be less affected by surface structures.

Another important feature of the maximum yield stress is that the maximum yield stresses of silica–lysozyme suspensions in 10 mM KCl are larger than the yield stresses of bare silica suspensions in 0.5 M KCl, although the KCl concentration is low (see Figure 3). Needless to say, we could not detect the yield stress of suspensions of bare silica particles in 10 mM KCl at pH 5 and 7. According to the DLVO theory, electric repulsion between silica particles decreases with an increase in the ionic strength owing to the compression of the electric double layer. Previously, Franks [43] demonstrated that the yield stress of silica suspensions either increased or remained with ionic strength increase. Therefore, our observation of higher maximum yield stresses of mixed suspensions of lysozymes and silica particles compared to the yields stress of bare silica particle suspension with 0.5 M KCl cannot be explained in terms of the specific features of bare silica particles reported by Franks or the DLVO theory. Thus, additional attractive forces must exist, such as bridging and patch attraction. Furthermore, these additional attractive forces induce the pH dependence of the maximum yield stress as the surface properties of silica particles and lysozymes depend on pH.

According to the DLVO theory, yield stress depends only on the van der Waals force and electric double layer force, and is characterized by the zeta potential. Thus, if one plots yield stresses against zeta potentials, the graphs become symmetrical with respect to the iep. However, in Figure 3, the graphs are asymmetrical with respect to the iep. At pH 5, the difference between the negative and positive zeta potential is insignificant. At pH 7, the range of the detected yield stresses is wider when the zeta potential is negative as compared to its counterpart when the zeta potential is positive. These results indicate the existence of additional forces that depend on the adsorbed amount of lysozymes and pH. We consider that these additional forces include patch attraction, bridging, and lateral repulsion between adsorbed lysozymes.

To examine the effect of the adsorbed amount of lysozymes on particle–particle interactions, we introduce the relative adsorbed amount, θ_{rel}, which is the ratio of the adsorbed amount Γ to the maximum adsorbed amount Γ_{max} under the same solution conditions. If a linear relation between the adsorbed amount and surface coverage is assumed, θ_{rel} can be obtained by $\theta_{rel} = \Gamma/\Gamma_{max} = \theta/\theta_{max}$ with the maximum surface coverage θ_{max}. Here, θ_{rel} may represent the fraction of occupied spaces, including the region where electrostatic repulsion occurs, and the probability of occurrence of patch–bridging attraction should be proportional to $\theta_{rel}(1 - \theta_{rel})$. In other words, at $\theta_{rel} = 0.5$, the patch–bridging attraction can be considered maximal, and when θ_{rel} is far from 0.5, the attraction may decrease owing to the small

probability of patch–bridging attraction and/or overlap of adsorbed lysozymes. The consideration on θ_{rel} is based on Smellie and La Mer's concept of the probability of bridging formation. However, in the present study, θ_{rel} is based on Γ_{max} to consider the electric repulsion between lysozymes. In Figure 5, the yield stresses are plotted against the relative adsorbed amount, θ_{rel}. The lines represent the relative adsorbed amounts corresponding to the iep. As shown in Figure 5, the maximum yield stresses at pH 5 and 7 are located around the isoelectric point instead of around $\theta_{rel} = 0.5$. This implies that, in mixed suspensions of oppositely charged lysozymes and silica particles, the relative adsorbed amount exhibits a smaller correlation with the yield stress than the zeta potential. However, the concept of relative adsorbed amount may explain the asymmetry between the yield stresses and zeta potential by the following consideration.

Figure 3 illustrates the relationship between yield stresses and zeta potentials at pH 5 and 7 and the schematic representations of the gap between silica particles under the corresponding conditions. The vertical lines represent the zeta potentials when the relative adsorbed amount θ_{rel} is 0.5. At pH 5 (Figure 3 (a)), the zeta potential is +8 mV at $\theta_{rel} = 0.5$. Thus, attractive forces occur between lysozyme-coated silica particles regardless of the zeta potential sign. Furthermore, the adsorbed amount of lysozyme is much smaller than that at pH 7. These adsorption profiles result in a symmetric DLVO-like or small asymmetric feature of yield stress with respect to the zeta potential at pH 5.

At pH 7 (Figure 3 (b)), $\theta_{rel} = 0.5$ is located near the iep. Thus, attractive forces between adsorbed lysozymes on a silica and the other silica surfaces exist when the zeta potential is negative. Meanwhile, when the zeta potential is positive, the adsorbed lysozymes may form a homogeneous layer on the silica surface. In this region, the adsorption density of lysozymes in the gap between silica particles reaches the maximum adsorbed amount. Therefore, repulsive forces exist between lysozymes on a particle and lysozymes on another particle. At pH 7, the additional attraction between silica particles covered with small amount of lysozymes ($\theta_{rel} < 0.5$) works in the range of negative zeta potential, while the repulsion between silica particles covered with larger amount of lysozymes ($\theta_{rel} > 0.5$) works at positive zeta potential regime. Therefore, the yield stresses are detectable in a wider zeta potential range when the zeta potential is negative.

It is known that the magnitude of yield stress is proportional to the square of the zeta potential. This linearity was observed in theoretical models [45,46], in which interparticle forces are expressed in terms of the DLVO theory, and has been confirmed experimentally [11,17,33]. At low lysozyme doses and pH 7, the plots of yield stresses against the square of the zeta potential are curved (see supporting information Figure S2). This observation supports the existence of additional non-DLVO forces such as patch–bridging attraction. Meanwhile, the linear relationship between the yield stresses and the square of the zeta potential at a high dose of lysozyme at pH 7 implies that the interaction between silica particles is DLVO like because of a homogeneous lysozyme layer on the silica surface.

4. Conclusions

To investigate the interactions between colloidal particles in the presence of proteins, the yield stresses of mixed suspensions of lysozymes and silica particles were measured as a function of lysozyme dose under two different pH conditions. The measured yield stresses were compared to surface properties that were characterized by the adsorbed amounts and zeta potentials. Our results indicated that the zeta potential was an important parameter in estimating the interactions, as expected from the DLVO theory. However, the zeta potential alone could not explain the several trends followed by the yield stresses, such as the pH dependence of the maximum yield stress and the different yield stresses at the same magnitude of zeta potential. These results confirmed the existence of non-DLVO forces, such as the patch–bridging attraction and lateral repulsion between adsorbed lysozymes. The relative adsorbed amount of lysozymes could explain the asymmetric feature of yield stresses with respect to the iep. The relationship between yield stresses and squares of zeta potentials suggested that a transition between DLVO-like and non-DLVO-like interactions occurred by the increase in adsorbed lysozyme amounts. Furthermore, the relative adsorbed amount could be used as a parameter to analyze the transition of interaction mechanisms and the existence of patch–bridging attraction and lateral repulsion between adsorbed lysozymes.

Acknowledgement

The authors are grateful for NIHON RUFUTO CO. and Dr. Shinichi Takeda kindly allowing us to use DT-1202. The authors are also very thankful to Dr. Pham Tien Duc for his advice for measurement of adsorbed amount. This study was financially supported by the JSPS KAKENHI (19H03070, 17J00332, 16H0638, and 15H04563).

References

[1] R. Cukalevski, S.A. Ferreira, C.J. Dunning, T. Berggård, T. Cedervall, IgG and fibrinogen driven nanoparticle aggregation, Nano Res. 8 (2015) 2733–2743. doi:10.1007/s12274-015-0780-4.

[2] U. Gassenschmidt, K.D. Jany, B. Tauscher, H. Niebergall, BiochimicaL et Biophysics &ta Isolation and characterization of a flocculating protein from Moringa oleifera Lam, Biochim. Biophys. Acta. 1243 (1995) 477–481. doi:10.1016/0304-4165(94)00176-X.

[3] S. Saallah, I.W. Lenggoro, Nanoparticles carrying biological molecules: Recent advances and applications, KONA Powder Part. J. 2018 (2018) 89–111. doi:10.14356/kona.2018015.

[4] B. V Derjaguin, L. Landau, Theory of stability of highly charged lyophobic sols and adhesion of highly charged particles in solutions of electrolytes, Acta Physico-Chimica USSR. 14 (1941) 58.

[5] E.J. Willem, J.T.G. Overbeek, J. Theodoor, G. Overbeek, Theory of the stability of lyophobic colloids, Courier Corporation, 1999.
[6] W.A. Ducker, T.J. Senden, R.M. Pashley, Direct measurement of colloidal forces using an atomic force microscope, Nature. 353 (1991) 239–241. doi:10.1038/353239a0.
[7] N. Helfricht, A. Mark, L. Dorwling-Carter, T. Zambelli, G. Papastavrou, Extending the limits of direct force measurements: colloidal probes from sub-micron particles, Nanoscale. 9 (2017) 9491–9501. doi:10.1039/C7NR02226C.
[8] S.H. Behrens, D.I. Christl, R. Emmerzael, P. Schurtenberger, M. Borkovec, Charging and Aggregation Properties of Carboxyl Latex Particles : Experiments versus DLVO Theory, Langmuir. 16 (2000) 2566–2575.
[9] M. Schudel, S.H. Behrens, H. Holthoff, R. Kretzschmar, M. Borkovec, Absolute Aggregation Rate Constants of Hematite Particles in Aqueous Suspensions: A Comparison of Two Different Surface Morphologies., J. Colloid Interface Sci. 196 (1997) 241–253. doi:10.1006/jcis.1997.5207.
[10] S.B. Johnson, G. V. Franks, P.J. Scales, D. V. Boger, T.W. Healy, Surface chemistry-rheology relationships in concentrated mineral suspensions, Int. J. Miner. Process. 58 (2000) 267–304. doi:10.1016/S0301-7516(99)00041-1.
[11] S.B. Johnson, A.S. Russell, P.J. Scales, Volume fraction effects in shear rheology and electroacoustic studies of concentrated alumina and kaolin suspensions, Colloids Surfaces A Physicochem. Eng. Asp. 141 (1998) 119–130. doi:10.1016/S0927-7757(98)00208-8.
[12] J. Gregory, Rates of flocculation of latex particles by cationic polymers, J. Colloid Interface Sci. 42 (1973) 448–456. doi:10.1016/0021-9797(73)90311-1.
[13] L. Alison, P.A. Rühs, E. Tervoort, A. Teleki, M. Zanini, L. Isa, A.R. Studart, Pickering and network stabilization of biocompatible emulsions using chitosan-modified silica nanoparticles, Langmuir. (2016) acs.langmuir.6b03439. doi:10.1021/acs.langmuir.6b03439.
[14] Y.-K. Leong, Inter-particle forces arising from adsorbed bolaform surfactants in colloidal suspensions, J. Chem. Soc. Faraday Trans. 93 (1997) 105–109. doi:10.1039/a604953b.
[15] M. Kobayashi, S. Yuki, Y. Adachi, Effect of anionic surfactants on the stability ratio and electrophoretic mobility of colloidal hematite particles, Colloids Surfaces A Physicochem. Eng. Asp. 510 (2016) 190–197. doi:10.1016/j.colsurfa.2016.07.063.
[16] Y.K. Leong, D. V. Boger, P.J. Scales, T.W. Healy, Interparticle forces arising from adsorbed surfactants in colloidal suspensions: An additional attractive force, J. Colloid Interface Sci. 181 (1996) 605–612. doi:10.1006/jcis.1996.0418.
[17] B.C. Ong, Y.K. Leong, S.B. Chen, Interparticle forces in spherical monodispersed silica dispersions: effects of branched polyethylenimine and molecular weight., J. Colloid

Interface Sci. 337 (2009) 24–31. doi:10.1016/j.jcis.2009.05.018.
[18] W. Lin, P. Galletto, M. Borkovec, Charging and aggregation of latex particles by oppositely charged dendrimers., Langmuir. 20 (2004) 7465–73. doi:10.1021/la049006i.
[19] L. Feng, Y. Adachi, A. Kobayashi, Kinetics of Brownian flocculation of polystyrene latex by cationic polyelectrolyte as a function of ionic strength, Colloids Surfaces A Physicochem. Eng. Asp. 440 (2014) 155–160. doi:10.1016/j.colsurfa.2012.09.023.
[20] Y. Adachi, L. Feng, M. Kobayashi, Kinetics of flocculation of polystyrene latex particles in the mixing flow induced with high charge density polycation near the isoelectric point, Colloids Surfaces A Physicochem. Eng. Asp. 471 (2015) 38–44. doi:10.1016/j.colsurfa.2015.02.011.
[21] Y. Adachi, A. Kobayashi, M. Kobayashi, Structure of colloidal flocs in relation to the dynamic properties of unstable suspension, Int. J. Polym. Sci. 2012 (2012). doi:10.1155/2012/574878.
[22] R.H.J. Smellie, V.K. La Mer, A Quantitative theory of filtration of flocculated suspensions, J. Colloid Sci. 23 (1958) 589.
[23] C. Zhao, G. Yuan, D. Jia, C.C. Han, Macrogel induced by microgel: bridging and depletion mechanisms, Soft Matter. 8 (2012) 7036–7043. doi:10.1039/c2sm25409c.
[24] R. Pericet-Camara, B.P. Cahill, G. Papastavrou, M. Borkovec, Nano-patterning of solid substrates by adsorbed dendrimers., Chem. Commun. (Camb). (2007) 266–8. doi:10.1039/b612249c.
[25] B.P. Cahill, G. Papastavrou, G.J.M. Koper, M. Borkovec, Adsorption of poly(amido amine) (PAMAM) dendrimers on silica: importance of electrostatic three-body attraction., Langmuir. 24 (2008) 465–73. doi:10.1021/la7021352.
[26] K. Sofin´ska, Z. Adamczyk, M. Kujda, M. Nattich-Rak, Recombinant Albumin Monolayers on Latex Particles, Langmuir. 30 (2014) 250–258. doi:10.1021/la403715s.
[27] K. Kubiak-Ossowska, M. Cwieka, A. Kaczynska, B. Jachimska, P.A. Mulheran, Lysozyme adsorption at a silica surface using simulation and experiment: effects of pH on protein layer structure, Phys. Chem. Chem. Phys. 17 (2015) 24070–7. doi:10.1039/C5CP03910J.
[28] B. Bharti, J. Meissner, G.H. Findenegg, Aggregation of silica nanoparticles directed by adsorption of lysozyme., Langmuir. 27 (2011) 9823–33. doi:10.1021/la201898v.
[29] J. Meissner, A. Prause, B. Bharti, G.H. Findenegg, Characterization of protein adsorption onto silica nanoparticles: influence of pH and ionic strength, Colloid Polym. Sci. 293 (2015) 3381–3391. doi:10.1007/s00396-015-3754-x.
[30] D. Lerche, T. Sobisch, Evaluation of particle interactions by in situ visualization of separation behaviour, Colloids Surfaces A Physicochem. Eng. Asp. 440 (2014) 122–130. doi:10.1016/j.colsurfa.2012.10.015.

[31] S. Kumar, V.K. Aswal, P. Callow, PH-dependent interaction and resultant structures of silica nanoparticles and lysozyme protein, Langmuir. 30 (2014) 1588–1598. doi:10.1021/la403896h.
[32] Y. Huang, A. Yamaguchi, T.D. Pham, M. Kobayashi, Charging and aggregation behavior of silica particles in the presence of lysozymes, Colloid Polym. Sci. 296 (2018) 145–155. doi:10.1007/s00396-017-4226-2.
[33] A. Otsuki, Coupling colloidal forces with yield stress of charged inorganic particle suspension: A review, Electrophoresis. (2018) 1–12. doi:10.1002/elps.201700314.
[34] M. Kobayashi, S. Ooi, Y. Adachi, On the Yield Stress of Sheared Coagulated Suspensions, Proc. Hydraul. Eng. 46 (2002) 637–640. doi:10.2208/prohe.46.637.
[35] G. V Franks, S.B. Johnson, P.J. Scales, D. V Boger, T.W. Healy, Ion-Specific Strength of Attractive Particle Networks, Langmuir. 15 (1999) 4411–4420. doi:10.1021/la9815345.
[36] M. Kobayashi, Y. Adachi, S. Ooi, On the Steady Shear Viscosity of Coagulated Suspensions., Nihon Reoroji Gakkaishi. 28 (2000) 143–144. doi:10.1678/rheology.28.143.
[37] M. Kobayashi, M. Skarba, P. Galletto, D. Cakara, M. Borkovec, Effects of heat treatment on the aggregation and charging of Stober-type silica, J. Colloid Interface Sci. 292 (2005) 139–147. doi:10.1016/j.jcis.2005.05.093.
[38] W.F. Tan, L.K. Koopal, L.P. Weng, W.H. van Riemsdijk, W. Norde, Humic acid protein complexation, Geochim. Cosmochim. Acta. 72 (2008) 2090–2099. doi:10.1016/j.gca.2008.02.009.
[39] B. Jachimska, A. Kozlowska, A. Pajor-Swierzy, Protonation of lysozymes and its consequences for the adsorption onto a mica surface., Langmuir. 28 (2012) 11502–10. doi:10.1021/la301558u.
[40] A. Yamaguchi, M. Kobayashi, Quantitative evaluation of shift of slipping plane and counterion binding to lysozyme by electrophoresis method, Colloid Polym. Sci. 294 (2016) 1019–1026. doi:10.1007/s00396-016-3852-4.
[41] N.Q. Dzuy, D. V. Boger, Direct Yield Stress Measurement with the Vane Method, J. Rheol. (N. Y. N. Y). 29 (1985) 335–347. doi:10.1122/1.549794.
[42] J. Mewis, N. Wagner, Colloidal Suspension Rheology, Cambridge University Press, 2011. doi:10.1017/CBO9780511977978.
[43] G. V. Franks, Zeta potentials and yield stresses of silica suspensions in concentrated monovalent electrolytes: isoelectric point shift and additional attraction., J. Colloid Interface Sci. 249 (2002) 44–51. doi:10.1006/jcis.2002.8250.
[44] M. Kobayashi, F. Juillerat, P. Galletto, P. Bowen, M. Borkovec, Aggregation and charging of colloidal silica particles: effect of particle size, Langmuir. 21 (2005) 5761–5769.

doi:10.1021/la046829z.
[45] R.J. Hunter, S.K. Nicol, The dependence of plastic flow behavior of clay suspensions on surface properties, J. Colloid Interface Sci. 28 (1967) 250–259.
[46] P.J. Scales, S.B. Johnson, T.W. Healy, P.C. Kapur, Shear Yield Stress of Partially Flocculated Colloidal Suspensions, AIChE J. 44 (1998) 538–544. doi:10.1002/aic.690440305.

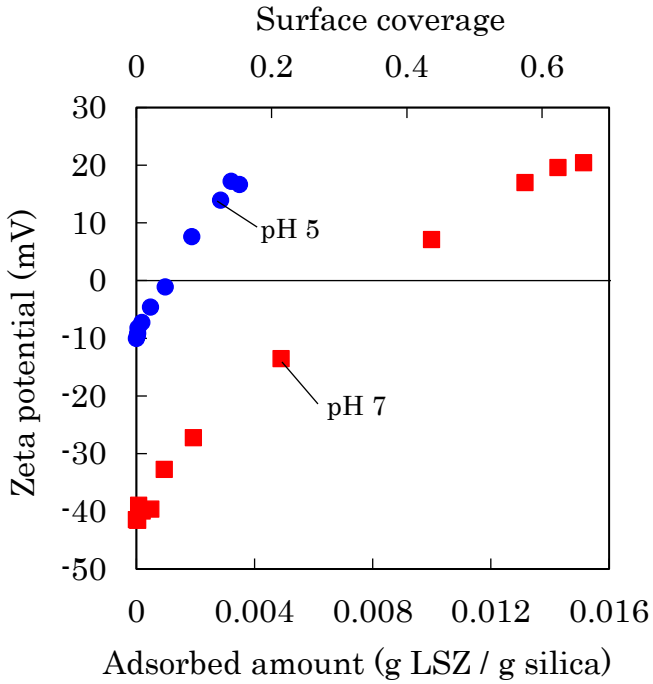

Figure 1 Zeta potential of lysozyme coated silica particles in 10 mM KCl at pH 5 and 7 are plotted against adsorbed amount (bottom) and corresponding surface coverage (upper).

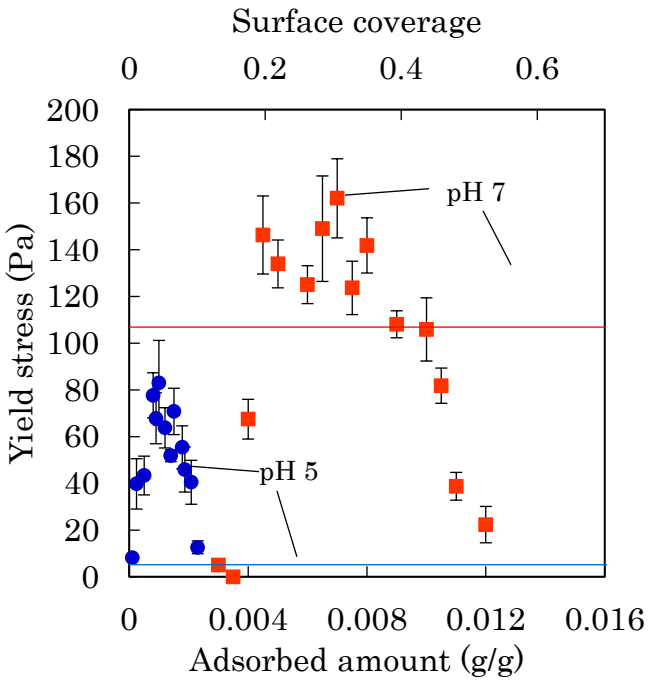

Figure 2 Yield stress of mixed suspension of lysozyme and silica particles at 10 mM KCl vs. adsorbed amount (bottom) and corresponding surface coverage (upper). The lines denote yield stress of silica suspension at 0.5 M KCl at pH 5 and at pH 7.

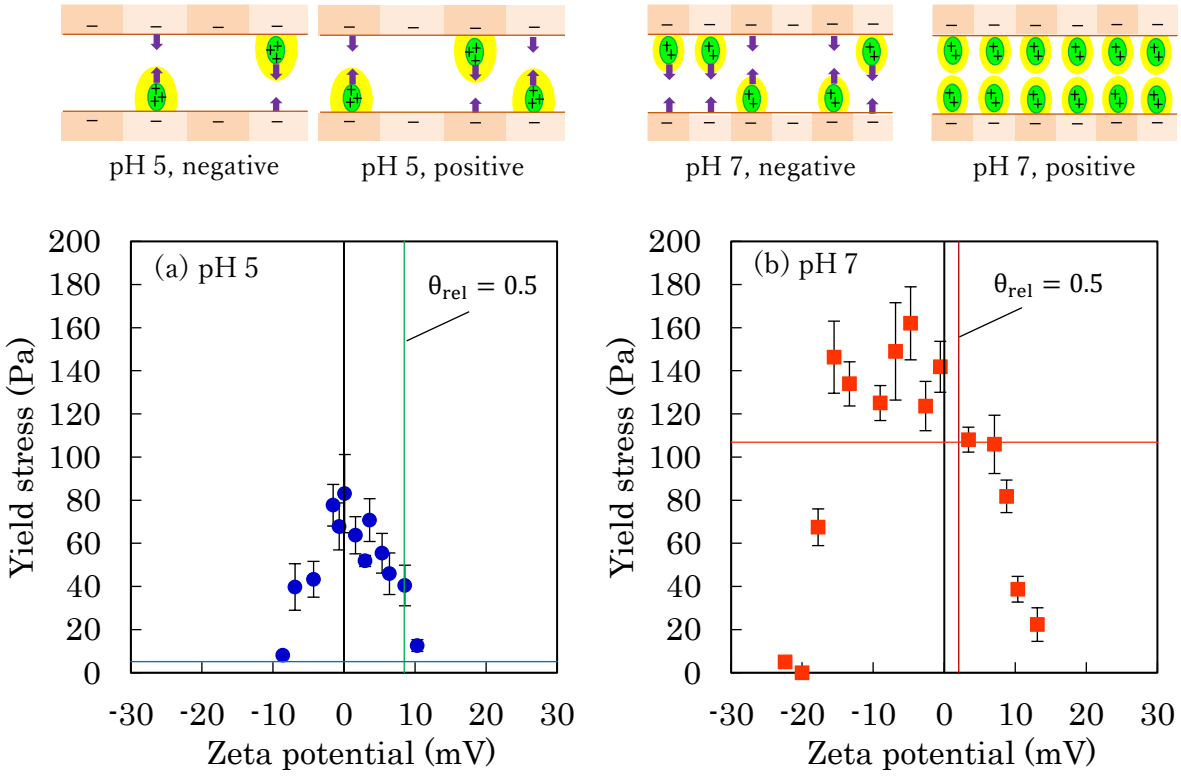

Figure 3 Yield stress of mixed suspension of silica and lysozyme at 10 mM KCl vs. zeta potential (a) at pH 5 and (b) at pH 7. The horizontal line is the yield stress of bare silica particle suspension with 0.5 M KCl. The vertical line is the zeta potential where the relative adsorbed amount equals to 0.5. The above pictures are schematic representation of gap between silica particles.

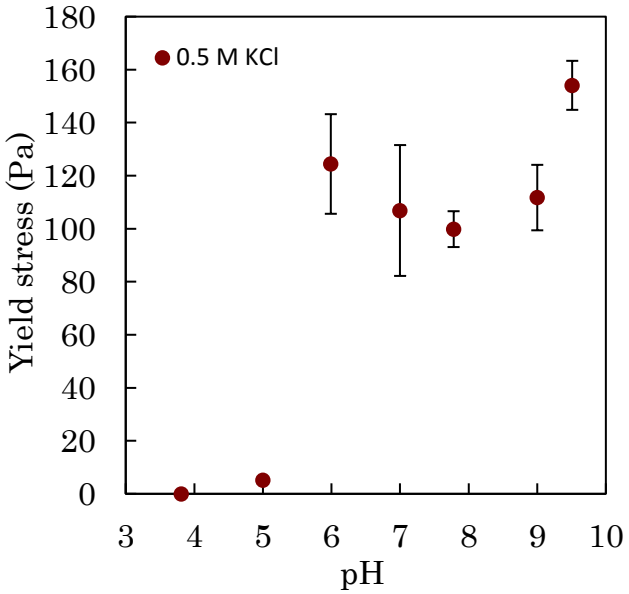

Figure 4 Yield stress of the suspension of bare silica particles at 0.5 M KCl vs. pH.

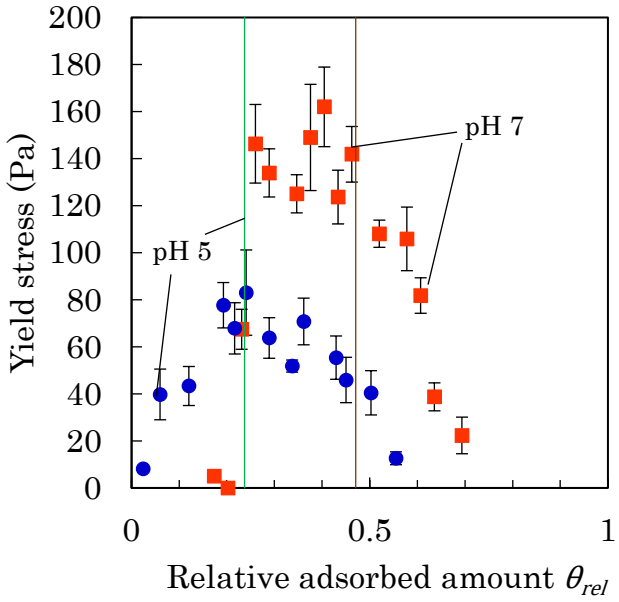

Figure 5 Yield stress of mixed suspension of lysozyme and silica at 10 mM KCl vs. relative adsorbed amount. The lines represent the relative adsorption mass corresponding to isoelectric point.